CHAPTER 3

MATERIALS AND METHODOLOGY

3.1 General

Performing field tests on a life-scale structure is generally very limited due to the size and scale of operations involved in executing them properly. Also, field tests are cost-intensive and involve large manpower deployment. As such, laboratory-scale physical modeling is considered an intuitive way to study the various aspects influencing the prototype behavior. A comprehensive description of the different raw materials used in this study has been given in this section. The various engineering properties of the materials obtained from laboratory tests have also been presented here. A detailed explanation of the model test setup, along with the sequence of the workflow during the entire work, is presented below:

- Procurement of raw materials.
- Fabrication of the model test setup.
- Basic testing of the materials to determine required physical and engineering properties.
- Preparation of the model test sample as per the testing scheme.
- Calibration of the loading and data acquisition systems, and the sensors.
- Performing static and cyclic load tests on soft soil clay bed improved by single GC and PGC.
- Static and cyclic tests on model embankment supported by GC and PGC reinforced clay bed.

The amount of literature available on full-scale tests on granular columns in the field is very limited. This could be attributed to the overall cost and the complexity involved in

the execution of the field tests. Laboratory-scale physical modeling has played a pivotal role in simulating the field test conditions at a reduced scale. The results of the model tests have been helpful in understanding the effect of various physical and specific structural parameters on prototype behavior. The understanding of granular column-improved soil foundations has been thoroughly explored for their application under static loading conditions. However, many of the GC applications involve its use in transport infrastructure development over soft soils. The loads acting on the transportation routes are cyclic in nature. The effect of the cyclic vehicular loads acting on the highway subgrade must be evaluated for a better understanding of the granular column behavior.

This chapter presents the model test scheme, scaling considerations, sample preparation, column installation, loading, and instrumentation procedure adopted for all the tests in the following sections and sub-sections.

3.2 Materials and methodology

3.2.1 Kaolinite clay

The use of kaolinite clay was done in this study for the formation of a soft clay bed in the model tests. A dry powdered form of commercially sourced kaolinite was obtained in plastic bags from the market. The properties of kaolin clay are presented in Table 3.1.

3.2.2 Sand

The sand used in this study for the formation of a sand mat over the clay bed is river sand procured locally. The grain size distribution of the sand material is given in Fig. 3.1. Poorly graded sand was used to provide a cushion layer below the footing. The shear strength parameters were determined using direct shear tests. The relevant

physical and engineering properties of the sand material determined from laboratory tests are presented in Table 3.2.

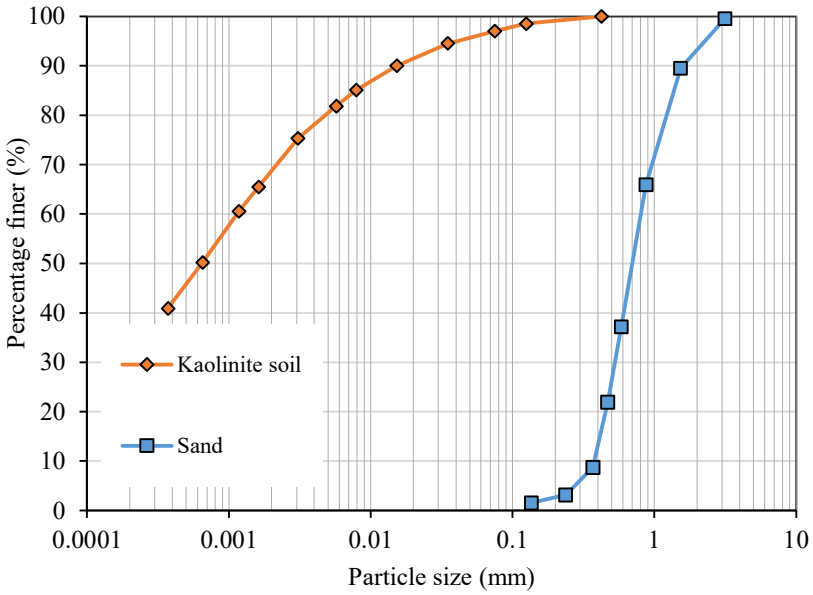

Fig. 3.1 Grain size distribution of kaolin clay and sand.

Table 3.1 Properties of kaolin clay.

Parameters	Value
Liquid limit, w_l (%)	49
Plastic limit, w_p (%)	22
Plasticity index, I_p (%)	27
Specific gravity, G_s	2.62
Optimum moisture content (%)	18.5
Maximum dry density (kN/m^3)	16.03
Coeff. of permeability (m/s)	6.75×10^{-10}
Soil classification (USCS)	CL

The variation of undrained shear strength, S_u of the kaolin clay with moisture content, was determined by performing vane shear tests in the laboratory. It can be observed from the plot in Fig. 3.2 that the undrained shear strength varies from 5 kPa – 15 kPa for water content varying from 35 % to 42 %.

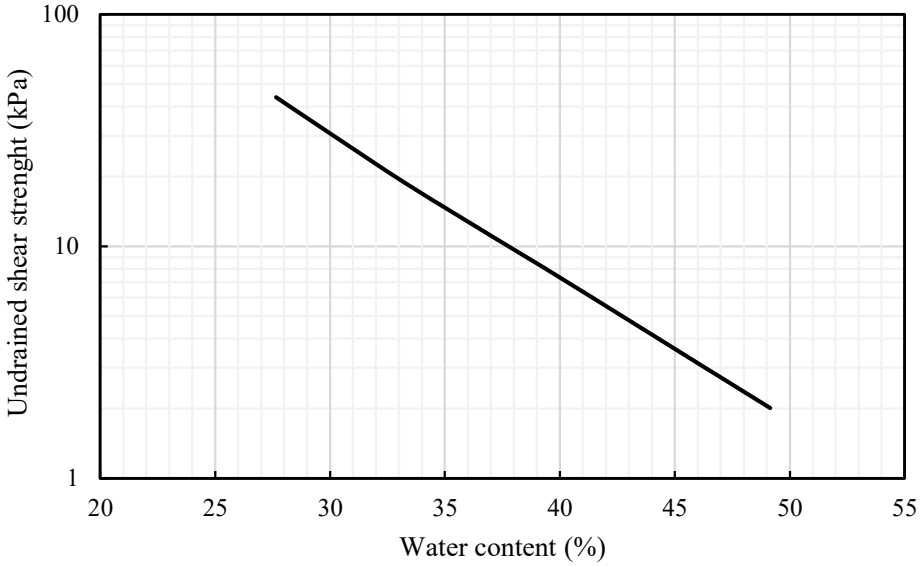

Fig. 3.2 Variation of undrained shear strength with water content.

Table 3.2 Properties of sand.

Parameter	Sand
Specific gravity, G	2.65
Maximum unit weight	17.5
Minimum unit weight	14.6
Angle of internal friction, ϕ	36
Uniformity coefficient, C_u	1.75
Curvature coefficient, C_c	3.57
Soil classification (USCS)	SP

3.2.3 Aggregates and plastic granules

Locally available stone aggregates, typically used in construction activities, were procured to form the columns. The size of the aggregates ranges from 2 mm to 6 mm. Acrylonitrile butadiene styrene (ABS) plastic waste materials, pelletized into plastic granules, had been procured locally from commercial suppliers. The plastic granules were selected such that they had a gradation similar to the stone aggregates. The granular materials used in this study are shown in Fig. 3.3. The grain size distribution of the stone aggregates and plastic granules is presented in Fig. 3.4. The engineering properties of the materials obtained from laboratory tests are shown in Table 3.3.

Table 3.3 Properties of stone aggregates and plastic granules.

Parameter	Aggregate	Plastic granules
Specific gravity	2.60	1.15
Maximum dry unit weight (kN/m^3)	16.6	9.57
Minimum dry unit weight (kN/m^3)	14.12	7.82
Angle of internal friction, ϕ	45	43
Dry unit weight at 65% relative density (kN/m^3)	15.64	8.87

(a) (b)

Fig. 3.3 Materials used in the study: (a) plastic granules, (b) stone aggregates.

3.2.4 Embankment soil

Silty sand was used as a fill material for the construction of the embankment, as recommended in RDSO guidelines. (RDSO 2020). The grain size distribution curve of silty sand is shown in Fig. 3.4. The properties of the embankment material determined from the laboratory test are presented in Table 3.4.

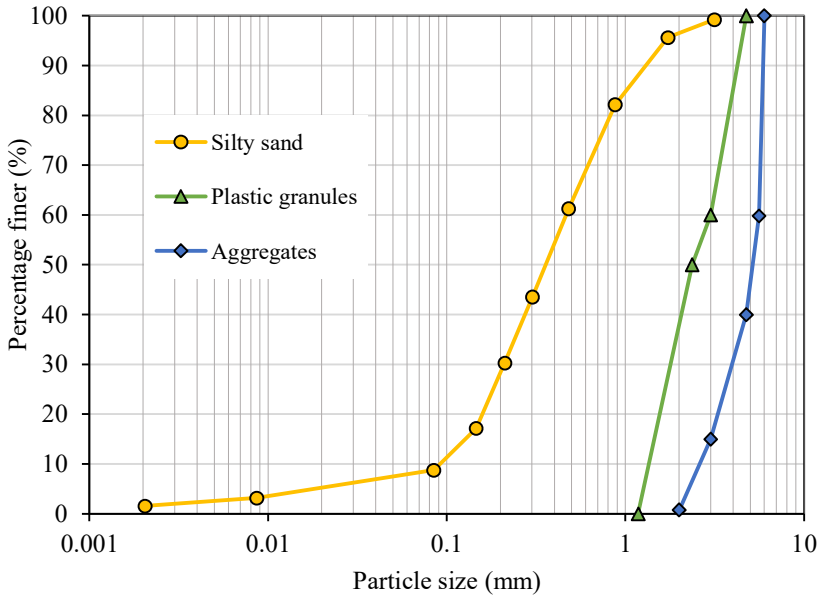

Fig. 3.4 Grain size distribution of embankment soil, aggregates, and plastic granules.

Table 3.4 Properties of embankment soil.

Parameters	Value
Specific gravity, G_s	2.67
Maximum dry density (kN/m^3)	18.32
Optimum moisture content (%)	9.5
Angle of internal friction, φ (degrees)	35

3.2.5 Geosynthetic encasement

A polypropylene biaxial geogrid material is used for encasing the columns. The geogrid material and its role as an encasement are shown in Fig. 3.5. The wide-width test was performed on the geogrid as per ASTM code D4595 (ASTM 2015) to determine its tensile strength as shown in Fig. 3.6. A tensile strength of 16 kN/m was observed at a plastic strain of 11 % as shown in Fig. 3.7. The tensile test on the geogrid material is depicted in Fig. 3.6.

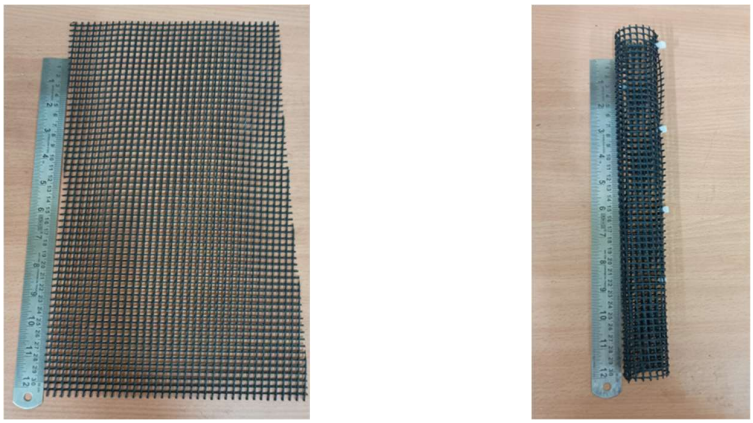

(a) (b)

Fig. 3.5 Geosynthetic material used in the study: (a) geogrid, (b) geogrid encasement.

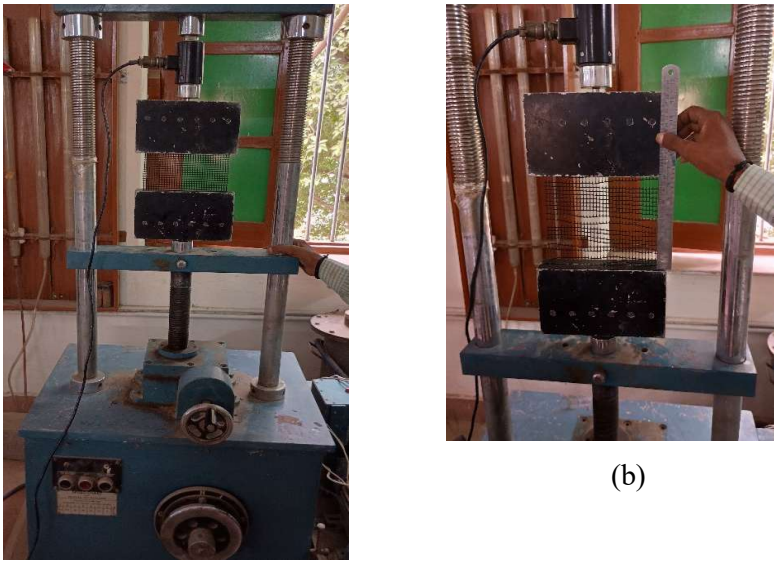

(a) (b)

Fig. 3.6 Tensile strength test on geogrid material, (a) before failure, (b) after failure.

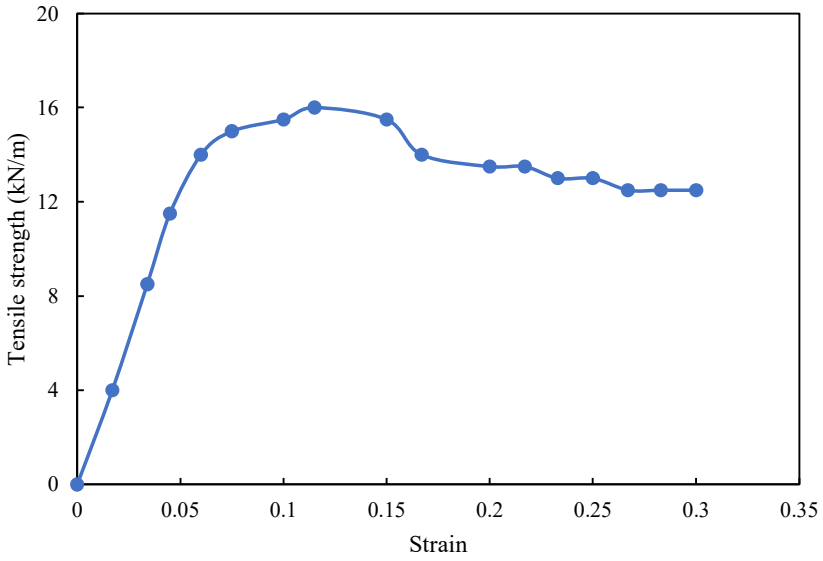

Fig. 3.7 Tensile strength vs strain relation of the geogrid.

3.3 Model tests on single granular column foundation

3.3.1 Test setup

A set of small-scale laboratory model tests were performed in a square tank with inner sides of 300 mm, height of 500 mm, and thickness of 5 mm, as shown in Fig. 3.8 (a). To prevent the tank from moving laterally while being loaded, the sides were restricted. The dimensions of the model test tank were considered based on necessary boundary conditions so that no interference would occur between the sides of the tank and the failure zone of the granular column, as shown in Fig. 3.8(b). To achieve this, (Meyerhof and Sastry 1978) recommended that the failure zone extend over the radial distance of about 1.5*d* from the periphery of the column, where *d* is the diameter of the column. For the column with a maximum diameter of 40 mm, 1.5*d* is 60 mm from the periphery of the column. Moreover, (Ali et al. 2012; Shahu and Reddy 2011) recommended that the tank boundaries should be chosen such that the induced stresses should become insignificant (<10%) at the tank boundaries. The selected dimensions of the tank ensure that the stresses generated at its borders are not greater than 10% of the

loads applied to the footing. The stress distribution was calculated considering an equivalent footing placed at two-thirds depth from the top of the column, as presented in Fig. 3.8 (b). It can be seen that the 2V:1H stress distribution does not reach the tank boundaries, so the stresses at the boundaries become insignificant.

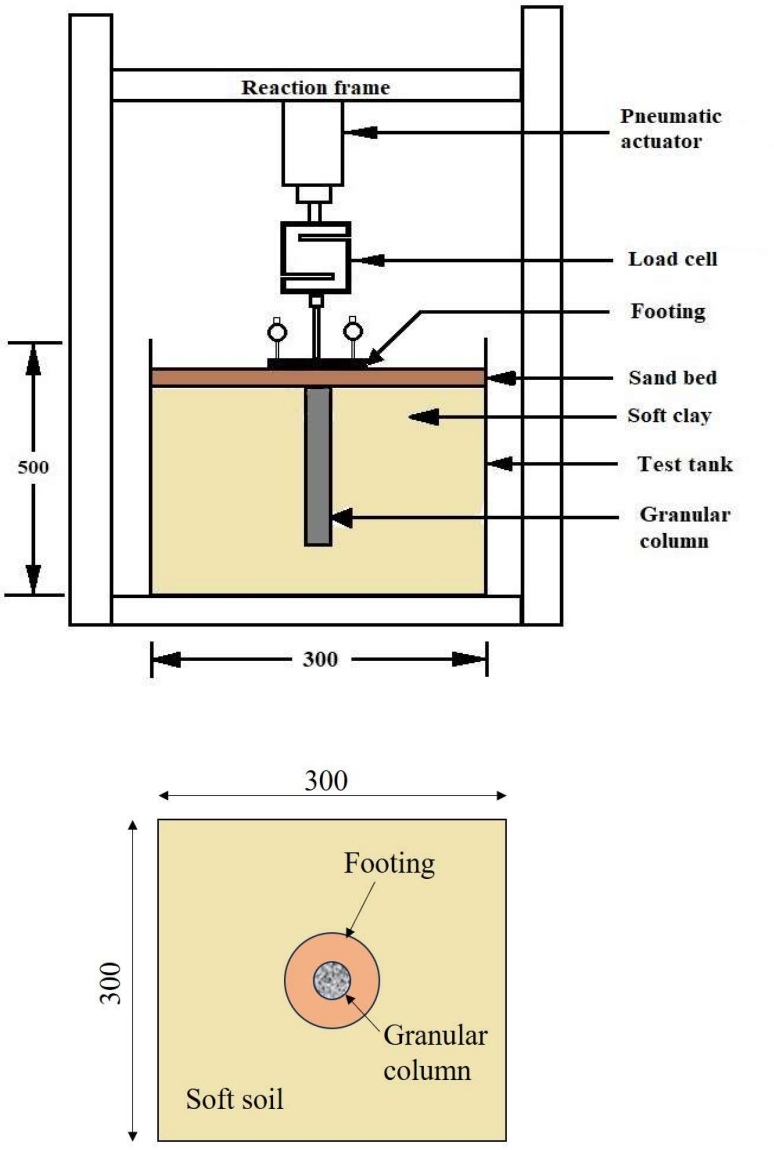

(a)

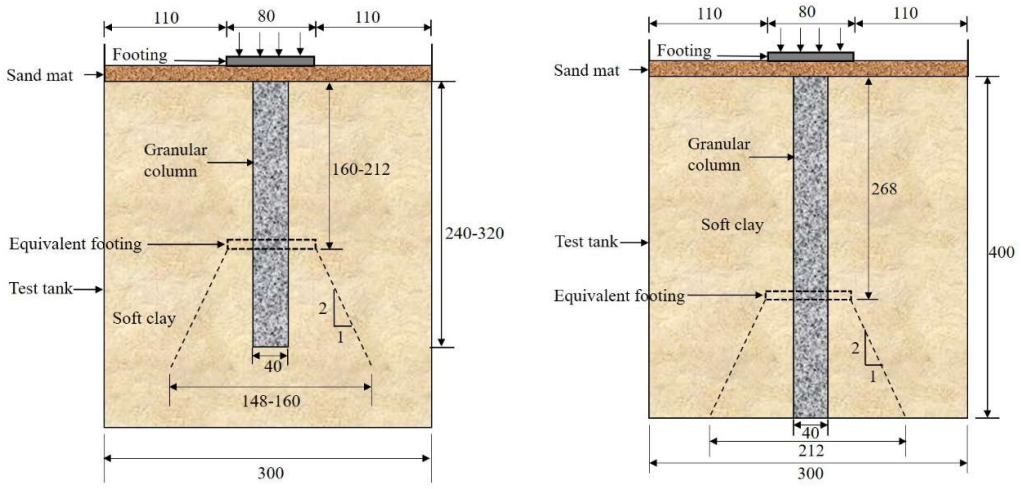

(b)

Fig. 3.8 (a) Model test setup along with the location of earth pressure sensors and pore pressure transducers, (b) criteria for selection of tank size.

3.3.2 Scaling considerations

The test tank used in this study had a width of 300 mm, 300mm in length, and 500mm in height. This size of the test tank was selected based on the considerations discussed earlier. A schematic view of the tank, clay bed, and columns within the soil mass is depicted in Fig. 3.8(b).

The scaling methods adopted by Wood (2000) were considered for comparative analysis of the model tests. A 40 mm column diameter was selected to represent a granular column of 0.6 m diameter, corresponding to a scale ratio of 15. The size of the aggregates used in the model tests was such that the ratio of the column diameter to the aggregate size was similar to that adopted in the field. Granular aggregates of mean particle size d_{50}= 3.6 mm and recycled plastic granules of mean size d_{50}= 3.1 mm reflect a column diameter to particle size ratio of 11-12.5, which are well in conformity with corresponding prototype foundations in soil (Shahu and Reddy 2011).

The length of the columns used in this study was 6, 8, and 10 times its diameter for the floating and end-bearing conditions. The length-to-diameter ratio of the prototype

columns varies in the range of 5-20 (Shahu and Reddy 2011). The granular materials used in this study were scaled as per the approach used by Wood (Wood et al. 2000). The ratio of granular column diameter to the mean size of the aggregates was found to vary between 8-40 for prototype dimensions (Debnath and Dey 2017; Jamshidi Chenari et al. 2019; Murugesan and Rajagopal 2010; Pradeep et al. 2024). The size of the granular materials used in this study was selected so that the column diameter and mean particle size follow a similar ratio as typically adopted in the field. The column diameter of 40 mm and mean particle size of 3.1 mm and 3.6 mm of the aggregates reflect a similar ratio. The scaling law used in this study is stated in Table 3.5.

Table 3.5 Similitude law for model tests against prototype.

Variables	Dimension	Scale factor
Length	m	λ
Area	m^2	λ^2
Density	kg/m^3	1
Stress	kPa	1
Force	kN	λ^2
Strain	m/m	1

3.3.3 Preparation of clay bed and column installation

Granular column is an effective ground improvement technique to improve the strength of soft soils with undrained shear strength, S_u, of less than 25 kPa. Considering this, the model tests were performed on a soft soil bed with undrained shear strength of 5-15 kPa. Several trails of vane shear tests were conducted to determine the water content required to prepare a soft soil bed at targeted shear strength. Approximately 35% to 42% (± 1%) water content was added to oven-dried dry kaolin clay to achieve the target shear strength. The amount of water required is obtained from the undrained

shear strength vs. water content plot shown earlier in Fig. 3.2. A uniform soil paste was prepared using a mechanical mixer. To achieve a uniform and consistent moisture distribution throughout, the prepared paste was placed to rest for 24 h. by covering it with a damp jute cotton fabric. Before filling the tank with soft soil, the inner sides were coated with silicon grease and covered with a polythene sheet to minimize side-wall friction. The paste was placed in four layers of thickness. Each layer was thoroughly compacted and molded to remove any entrapped air voids. The tank was then covered with a moist cloth to avoid any moisture loss and left undisturbed for twenty-four hours to regain the thixotropic strength.

The procedure to prepare and install granular was considered from the previously reported research (Black et al. 2007; Ghazavi and Nazari Afshar 2013; Yoo and Abbas 2020). Columns were prepared using stone aggregates and plastic granules. To produce a model of column-reinforced soft clay, the location of the column was marked on the clay bed. A 300 mm x 300 mm wooden sheet was used as a guiding system for the installation of the column. The wooden sheet with a hole of the required diameter at the center, as per the test conditions, was kept on the soil bed to ensure that the PVC pipe and the column were vertically inserted into the soil. A spirit level was used to ensure that the pipe penetrated vertically into the model ground. A thin open-ended PVC pipe of 1 mm thickness and an internal diameter equal to the targeted column diameter is slowly inserted vertically without disturbing the nearby soil up to a depth of 50 mm. To minimize the effect of friction between soil and pipe, the inner and outer sides of the pipe were coated with oil. The soil inside the pipe was removed with the help of an auger, and the pipe was further pushed into the soil bed, this process was repeated till the desired depth of column installation was achieved. The amount of granular material for the formation of a column with 65 % relative density was

determined. Through multiple trials of the column installation process, it was observed that achieving a relative density of more than 65 % was difficult as the desired column dimensions could not be adhered due to the soft nature of the soil. The column material was poured into the excavated hole in four batches of equal weights, and each layer was compacted using a rammer. The pipe was gradually retracted by maintaining a 10 mm overlap with the material. This process repeated till the entire length of the column was installed. The complete process of soil bed formation and column installation is shown in Fig. 3.9. The column was left within the soil bed overnight to obtain homogeneous contact between the soil and the column. Finally, a sand mat with a 20 mm thickness was placed on the top of the model ground to transfer the load from the footing to the granular column and the surrounding soil.

The process discussed above was used for the installation of non-encased GC and PGC. The installation of geosynthetic encased columns followed a similar approach where the geogrid material was wrapped in the form of an encasement around the pipe by maintaining an overlap of 20 mm (Gniel and Bouazza 2009). The adjoining ends of the encasement material were stitched manually using nylon zip ties shown in Fig. 3.5 (b). Similar techniques were used for the formation of geosynthetic encasement by (Muni Pradeep and Kumar 2024; Yoo and Abbas 2019).

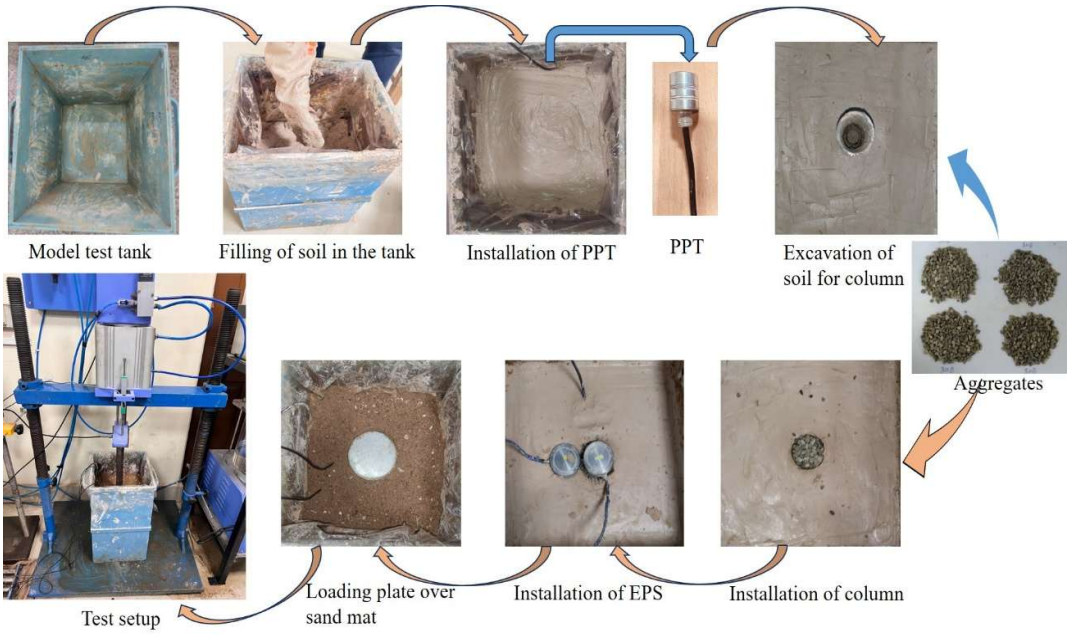

Fig. 3.9 Systematic diagram of the model test tank preparation and GC or PGC installation.

3.3.4 Instrumentation and Loading Procedure

In this model test, one small-sized pore-pressure transducer with a capacity of 50 kPa and two earth pressure sensors with a capacity of 200 kPa and 1 MPa were installed in the tank. The pore pressure transducer was installed to detect the pore water pressure while making the soil bed. The earth pressure sensors were installed after column installation. The 200 kPa earth pressure cell was installed above the soft soil bed, and a 1 MPa earth pressure cell was installed above the column to measure the load acting on the column and the surrounding soil. The exact location of these sensors is shown in Fig. 3.9. A DEWESOFT universal data gathering system was used to store and retrieve data from PPT and EPCs.

Static and cyclic loads were applied using a multifunctional, servo-controlled pneumatic loading data acquisition device with a 20 kN capacity. Using an LVDT connected to a data logger, the settlement of the footing was measured. The details of

all the instruments used in the study are presented in Table 3.6. All equipment, including the load cell, LVDT, and sensors, were calibrated properly before each model test.

Table 3.6 Technical specifications of geotechnical instrumentation.

Sensor name	Measurement	Capacity
Load cell	Load	20 kN
LVDT	Settlement	±50 mm
Earth pressure cell 1 (EP1)	Dynamic earth pressure	200 kPa
Earth pressure cell 2 (EP2)	Dynamic earth pressure	1 MPa
Pore pressure transducer (PPT)	Porewater pressure	50 kPa

The model test setup, along with the pore pressure transducer, earth pressure cell, and data logger, is shown in Fig. 3.10.

3.3.5 Load application under static condition

The model tests subjected to static loading were conducted in strain-controlled mode at a vertical settlement rate of 1.2 mm/min. The rate was chosen to simulate the undrained condition during loading (Hasan and Samadhiya 2017; Shahu et al. 2024).

The footing was subjected to a maximum settlement of 50 mm due to the limitation of the maximum movement of the actuator's piston. Furthermore, (IRC-37 2018) specifies a 20 mm maximum permissible surface deformation (rutting), which falls within the settlement range examined in the current study. The load applied on the footing and the corresponding settlement was measured using a load cell and an LVDT.

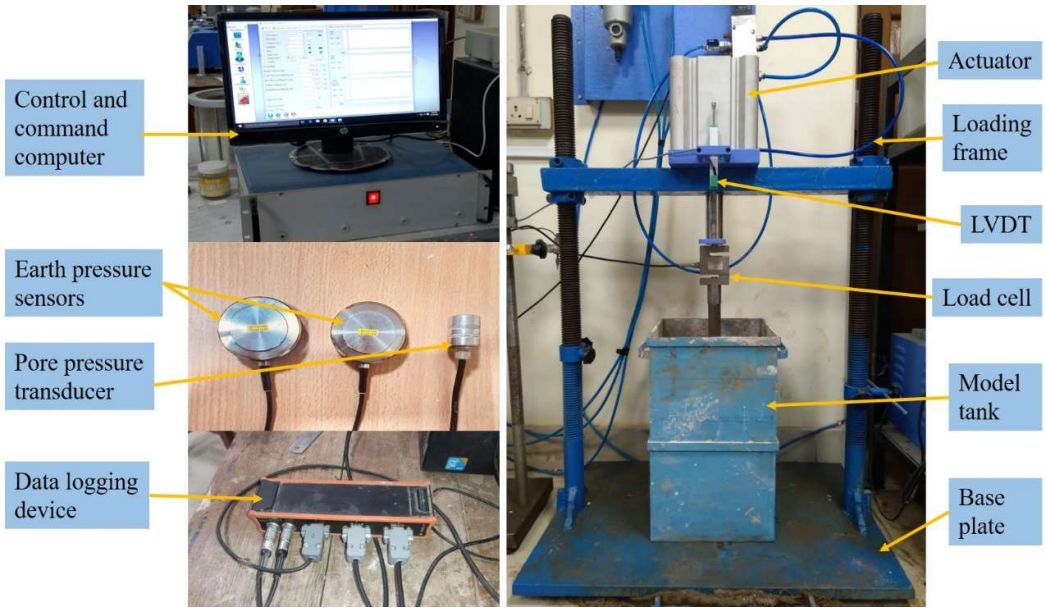

Fig. 3.10 Model test setup along with data loggers, earth pressure cells, and pore pressure transducer.

3.3.6 Load application under cyclic condition

The cyclic loading tests were performed in a load-controlled mode in the one-way sinusoidal cyclic form at a frequency of 1 Hz for 1000 cycles in each stage of loading until failure, whichever is reached earlier. The typical variation of the results obtained from the stress-controlled cyclic model test is shown in Fig. 3.11. Prior research has reported a slight impact of the frequencies in the 0.1 to 10 Hz range on the accumulated vertical strain pore water pressure (Liu and Xiao 2010; Toyota and Takada 2021). Cyclic loading was applied in a load-controlled mode in a sinusoidal (only compression) waveform to simulate the cyclic loading of a railway embankment. The cyclic stress induced by the movement of trains over railway tracks was taken into consideration for the evaluation of the dynamic behavior of railway embankments in this study. The estimated cyclic stress (σ_v) on the railway embankment is calculated using the empirical equation proposed by Ashour (Ashour et al. 2022).

$$\sigma_v = 0.26L\ (1+\alpha\ V) \tag{3.1}$$

The speed V (km/hr) and axle load L (kN) of the trains are considered when calculating the cyclic stress amplitude. A speed coefficient α of 0.004 was adopted for trains, as suggested by (Ashour et al. 2022) and (Pradeep et al. 2024). As per the Ministry of Railways, Government of India, the axle load of trains varies from 17.5 T to 25.T for semi-speed passenger trains to heavy haul goods trains. The maximum operating speed of passenger trains is 160 km/h, whereas the maximum speed of goods trains is 100 km/h. From the above empirical equation, it has been found that the induced dynamic stresses are in the range of 40 kPa to 90 kPa. A normalized parameter designated as cyclic stress ratio (CSR) was adopted to evaluate the effect of cyclic load on the granular column-reinforced soft clay bed. The CSR is calculated as:

$$CSR = \frac{q_c}{q_s} \tag{3.2}$$

where q_c is the cyclic loading amplitude, and q_s is the ultimate bearing capacity of the column-improved soil under static loading. The ultimate bearing capacity of a GC-improved soil with an A_r of 25% from static loading tests is determined as 78.53 (80 kPa). Past research reported that under cyclic loading, the critical stress is about 50% of the failure stress under monotonic loading, i.e., CSR = 0.5 (Ashour et al. 2022; Frost et al. 2004). Taking CSR of 0.5 for A_r of 25% gives a cyclic loading amplitude of 40 kPa. Four cyclic stress amplitudes with CSR values of 0.5, 0.7, 0.9, and 1.1 corresponding to stress values of 40 kPa, 56 kPa, 72 kPa, and 88 kPa were adopted for the 4-stage cyclic loading process. Previous studies used similar cyclic stresses varying in the 40-120 kPa range (Pradeep et al. 2024; Yoo and Abbas 2019; Zhang et al. 2020). Considering the cyclic stresses induced under traffic and train loading, this study takes the cyclic load amplitudes up to 90 kPa to simulate field cyclic stress conditions. A frequency of 1 Hz was chosen for cyclic loading in the present study to simulate loading conditions in the field based on studies done in the past (Gao et al. 2021; Xu et al. 2024).

Studies done in the past have reported that the cumulative strains developed in soft soils are independent of cyclic load frequencies in the range of 0.5-3 Hz (Ashour et al. 2022) and 0.1-10 Hz (Toyota and Takada 2021).

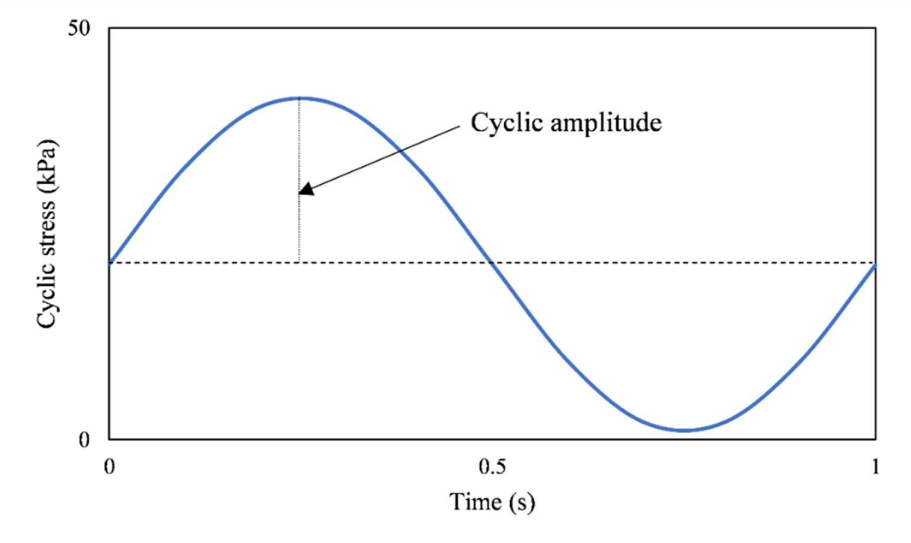

(a)

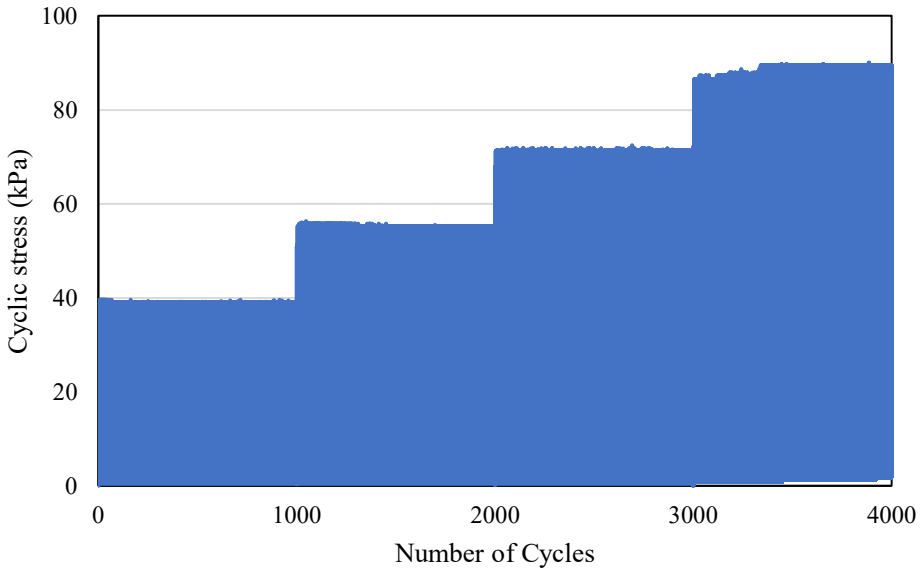

(b)

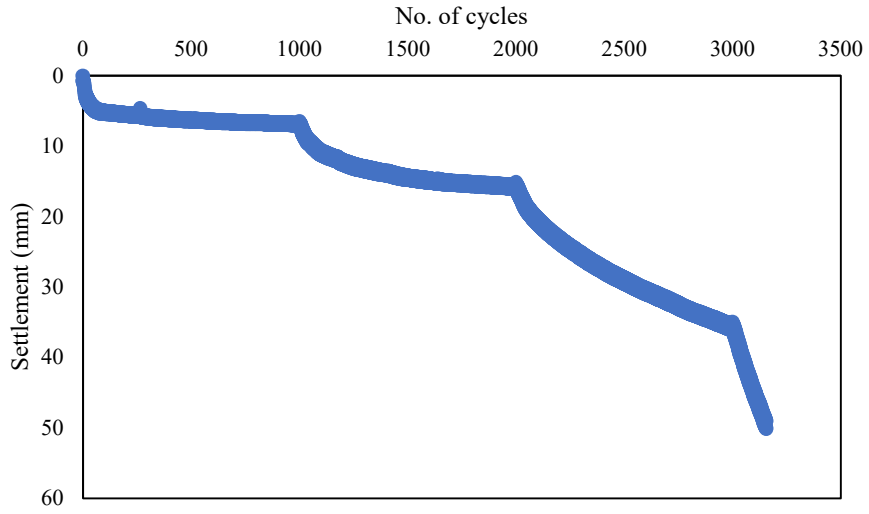

(c)

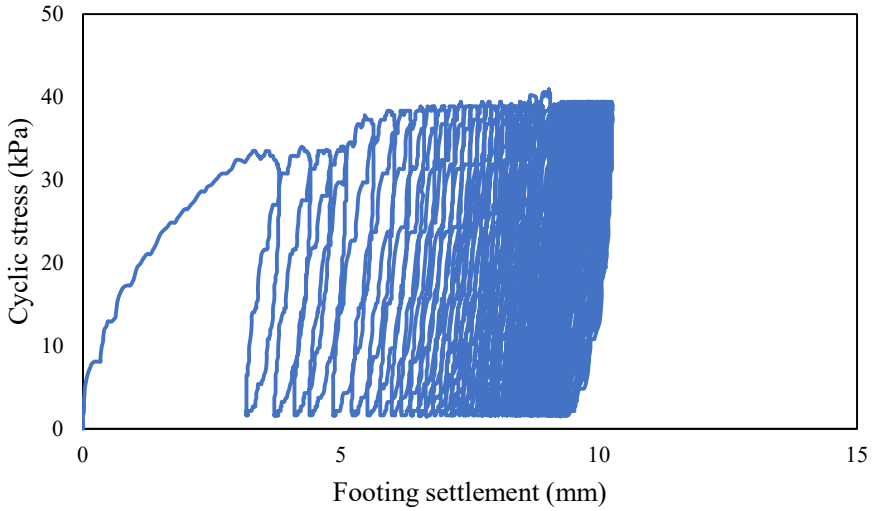

(d)

Fig. 3.11 (a) Variation of cyclic stress (q_c) pattern with number of cycles (N), (b) typical variation of q_c with N from the stress-controlled multi-staged cyclic model tests, (c) variation of footing settlement with number of cycles, and (d) variation of q_c with footing settlement.

3.4 Model tests on embankment over a group of columns

3.4.1 Details of test

This study discusses laboratory tests that simulate a model embankment over a composite soil foundation with granular columns installed vertically at a uniform spacing in a soft clay layer in a rectangular group pattern and subjected to vertical loading. A total of sixteen experiments were conducted on the unimproved and improved soft soil model beds reinforced with encased and non-encased GC and PGC in floating and end-bearing configurations subjected to static and cyclic loading.

3.4.2 Test setup and modeling considerations

The test tank used in this study had a width of 200 mm, a length of 500mm, and a height of 550mm. A 5 mm-thick mild steel sheet was used to fabricate the model test tank per the volumetric dimensions mentioned above. The size of the test tank was selected considering a wedge-shaped (2:1 Vertical: Horizontal) distribution of stress from 2/3rd of the depth of column length below the footing, such that the tank boundaries do not disrupt the stress distribution (Ali et al. 2012). A schematic view of the tank, clay bed, and columns within the soil mass is depicted in Fig. 3.12. The front-facing panel of the test tank on one of its sides was made detachable, which helped in the easy removal of soil from the tank after the test and provided a way to examine the post-loading failure pattern of the soft clay and the granular columns. The behavior of the embankment constructed over a soft clay bed improved using granular columns was studied by preparing the model embankment with a scaling factor of 30. Similar scaling factors were used in previous model studies (Fattah et al. 2016; Ullah et al. 2022).

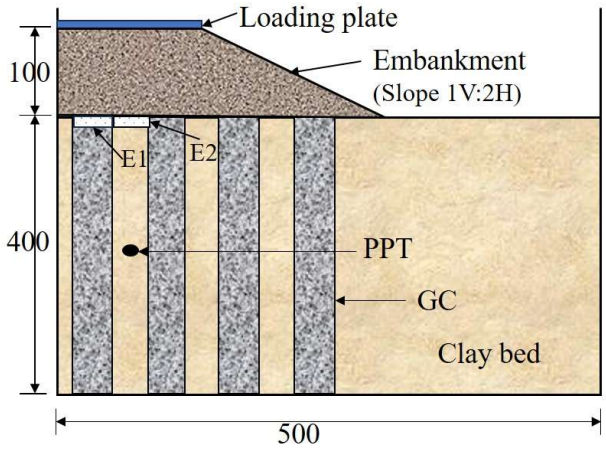

(a)

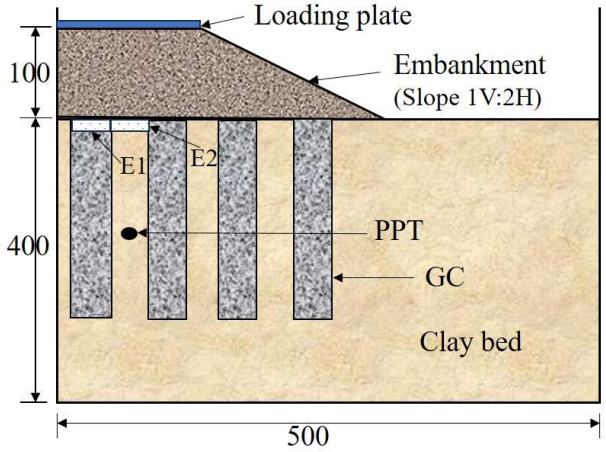

(b)

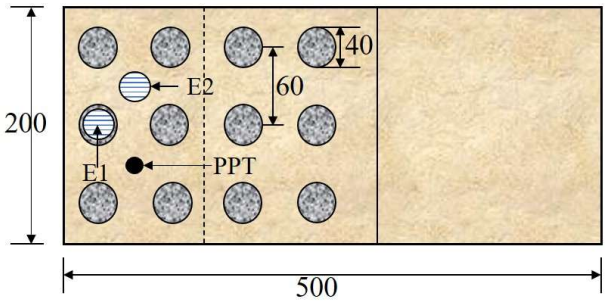

(c)

Fig. 3.12 Systematic view of the embankment model: (a) cross-sectional view of the end-bearing GCs, (b) cross-sectional view of the floating GCs, (c) plan view of GCs arrangement, respectively.

Because of the cross-sectional symmetry, only half of the embankment was modeled (Zheng et al., 2023). The embankment foundation was prepared using a 400 mm-thick soft clay bed. 40 mm diameter columns were installed to represent typical granular columns used in the field. The length of the columns used in this study was 8 and 10 times their diameter for the floating and end-bearing conditions. The length-to-diameter ratio of the prototype columns varies in the range of 5-20 (Shahu and Reddy 2011). The granular materials used in this study were scaled as per the approach used by Wood (Wood et al. 2000). The ratio of granular column diameter to the mean size of the aggregates was found to vary between 8-40 for prototype dimensions (Debnath and Dey 2017; Jamshidi Chenari et al. 2019; Murugesan and Rajagopal 2010; Pradeep et al. 2024). The size of the granular materials used in this study was selected so that the column diameter and mean particle size follow a similar ratio as typically adopted in the field. The column diameter of 40 mm and mean particle size of 3.1 mm and 3.6 mm of the aggregates reflect a similar ratio.

The height of the embankment was 83 mm, corresponding to the prototype embankment of 2.5 m height. A crest of 133 mm (prototype width of 4 m) was adopted, and a 1V:2H slope was provided. The columns were arranged in a rectangular grid pattern; the equivalent area ratio (A_r) was 25 %, as shown in Fig. 3.12 (c). The stresses applied in the model study were similar to those experienced in the prototype. Also, the cyclic loading frequency was adopted similarly to that in the prototype. This approach was adopted in previous studies on 1-g model tests (Aqoub et al. 2020; Li et al. 2023).

3.4.3 Model preparation and column installation

Soft soils generally have low undrained shear strength (< 25 kPa). A soft clay bed having an undrained shear strength of 10 ± 0.5 kPa was used in this study. Multiple trails of vane shear tests were carried out to ascertain the required water content to

generate a soft soil bed at the desired shear strength. Dry kaolin clay was mixed with approximately 37% water content to attain the desired shear strength. A mechanical mixer was used to make a homogeneous soil paste. The prepared paste was allowed to rest for a day to attain uniform and consistent moisture equalization. To avoid moisture loss, a damp jute bag was placed over it. To reduce side-wall friction, the inner sides of the tank were covered with a polythene sheet and silicon-greased before filling it with soft soil. The paste was added to the tank in Six layers, each layer of equal thickness thoroughly kneaded by hand to eliminate any trapped air voids. In order to prevent moisture loss, the tank was covered with a moist jute bag and left undisturbed for two days to restore its thixotropic strength.

The granular column installation and preparation process were adapted from previously published research work (Ali et al. 2012; Murugesan and Rajagopal 2010; Shahu and Reddy 2011). In order to achieve the required undrained shear strength, the oven-dried kaolin clay was initially mixed with the predetermined amount of water. A uniform paste of kaolin clay was prepared by mixing the soil in a mechanical mixer. After that, the paste was poured into a tray and left covered with a moist fabric for 24 hours for moisture homogenization.

To install the granular columns (GCs) inside the remolded soil bed in the model test tank, the locations of the columns were first marked on the clay bed. For this, wooden guiding plates with circular holes with a diameter of 40 mm with a spacing corresponding area replacement ratio of 25% arranged in a rectangular pattern were used. The wooden plate was held in a horizontal position above the model ground, and a thin open-ended PVC pipe with an outer diameter of the targeted diameter of the GC was then slowly pushed into each hole of the model ground up to the targeted depth. A leveling bubble was used to ensure that the pipe penetrated vertically into the model

ground. The PVC pipes were lubricated on the inside and outer surfaces. These pipes were gently pushed into the cay bed through the guide plate to a depth of 50 mm. The above sequence of operations was repeated till the required column depth. Stone aggregates or plastic granules were poured into the excavated hole in four batches. The column material poured into the hole was compacted to a relative density of 65%, determined by multiple trials as mentioned earlier. The PVC pipes were retracted after each filling while maintaining an overlap of 10 mm. This process was repeated a few more times till the whole length of the column was constructed. For the installation of EGC and EPGC, encasement tubes were placed in the PVC casing pipes before pouring the materials, and the rest of the procedure was similar to the procedure explained earlier.

The construction of the embankment fill was initiated after the installation of columns. Using a mixer, a predetermined weight of silty sand was combined with water to attain an optimum moisture content of 9.5 % and a maximum dry unit weight of 18.32 kN/m^3. The fill material was placed in multiple layers. Each layer was compacted using a tamping rod until the required embankment height was achieved. The model ground was left undisturbed overnight before the loading tests were conducted. The entire process involved in the formation of a soft clay bed, installation of columns, and the construction of the embankment for the model tests is illustrated with a systematic diagram shown in Fig. 3.13.

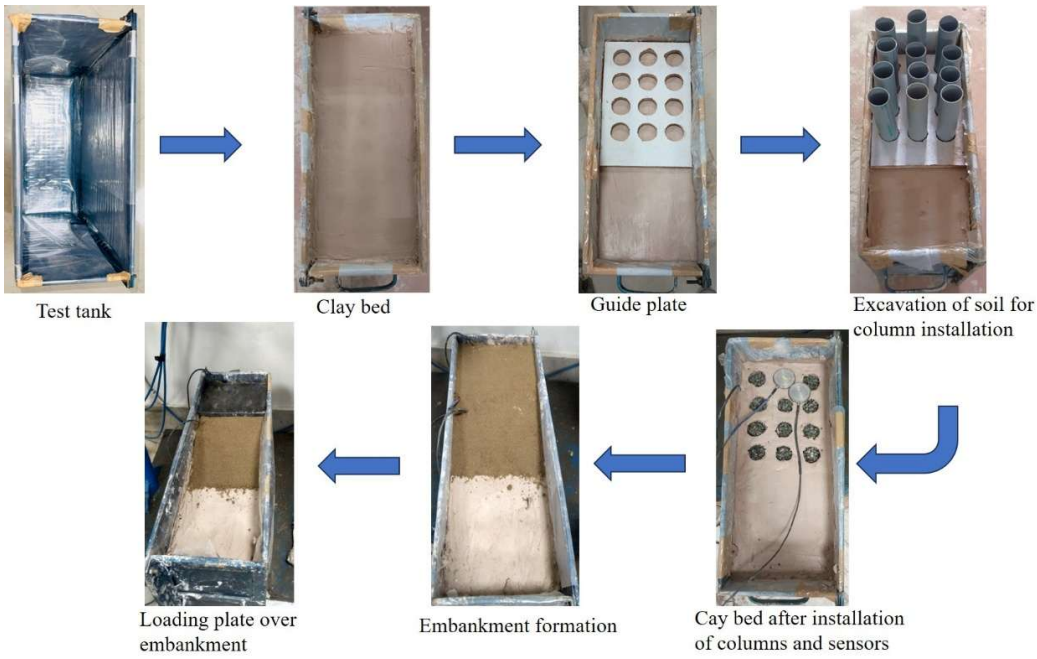

Fig. 3.13 Systematic diagram representing the installation of columns in clay bed and formation of embankment over the improved soil.

3.4.4 Instrumentation and loading procedure

One miniature pore pressure transducer with a capacity of 50 kPa and two earth pressure cells with capacities of 200 kPa and 1 MPa were installed in the tank for the model tests. The pore pressure transducer was installed while preparing the clay bed. The miniature pore pressure transducer (BPR-A-S, FSO-50 kPa making) was used to measure the excess pore pressure variation during the loading. Muni Pradeep and Kumar (2024) reported that the excess pore water pressure developed in the soil bed shows a higher value for measurement done in the top portion initially, which converges over time with the value observed by the sensor placed in the middle of the clay bed however lower excess pore pressure was recorded in the bottom section. The pore pressure sensor was placed in the middle of the cay bed to get reliable data. The pore pressor transducer weighed 50 grams, with a sensing surface diameter of 10 mm and a length of 20 mm. The pore water pressure is measured by a flexible silicon diaphragm

present in front of the pore pressure transducer. The diaphragm is protected from the surrounding soil by a ceramic filter at its front that allows only pore fluid to get through it. After the installation of the columns, the earth pressure sensors were placed on the top of the prepared model test surface. Similarly, two miniature earth pressure sensors, E1 & E2 (model KDE-200 kPa, KDE-1 MPa) from Tokyo Measuring Instruments Laboratories, were installed on the granular column and surrounding soil bed. The earth pressor sensors weighed 160 grams each, with a sensing surface diameter of 35 mm and a thickness of 11.3 mm. Fig. 3.12 (a) and 3.12 (b) display the exact position of these sensors. A multi-purpose, 20 kN capacity, servo-controlled pneumatic loading data acquisition system was used to apply static and cyclic loading. Fig. 3.14 shows the model test setup, data logger, pore pressure transducer, and earth pressure sensor. The displacement of the footing was measured using LVDT connected to the data logger.

Fig. 3.14 Model test setup.

The static loading tests were carried out in strain-controlled mode at a vertical displacement rate of 1.2 mm/min to simulate the undrained condition during loading.

The displacement rate was adopted based on studies reported in the literature for undrained loading conditions.

The cyclic loading tests were performed in a load-controlled mode in the one-way sinusoidal cyclic form at a frequency of 1 Hz for 1000 cycles of each stage until failure, similar to the cyclic loading on single-column model tests. Prior research has reported a slight impact of the frequencies in the 0.1 to 10 Hz range on the accumulated vertical strain and pore water pressure (Liu and Xiao 2010; Toyota and Takada 2021). (Lin et al. 2019) reported that traffic loading magnitude ranges between 40-90 kPa for different vehicles, from cars to fully loaded dump trucks on the roadway. Several studies have used cyclic stress amplitudes in the range of 30-100 kPa to simulate cyclic load acting on transportation routes. This study considered a cyclic stress intensity from 40-89 kPa to simulate the actual field loading condition. Fig. 3.15 (b) shows the typical vertical stress-settlement curve for 1000 cycles under four-stage load-controlled cyclic loading tests on the prepared models.

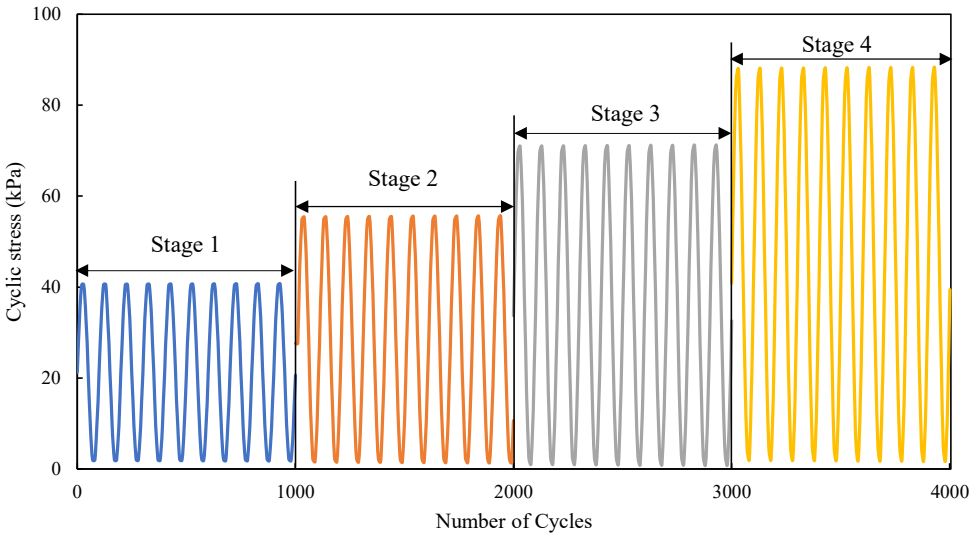

(a)

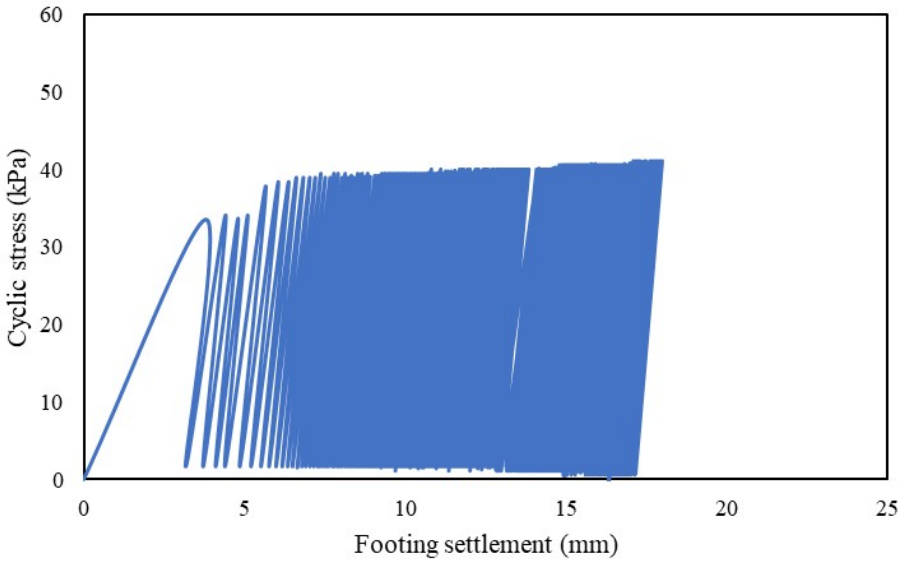

(b)

Fig. 3.15 (a) Cyclic loading stages with number of cycles, (b) typical variation of settlement under stage 1 cyclic loading.